

Neighborhood Homophily-based Graph Convolutional Network

Shengbo Gong

Institute of Cyberspace Security
Zhejiang University of Technology
Hangzhou, China

Binjiang Cyberspace Security Institute of ZJUT
Hangzhou, China
jshmhsb@gmail.com

Chenxuan Xie

Institute of Cyberspace Security
Zhejiang University of Technology
Hangzhou, China

Binjiang Cyberspace Security Institute of ZJUT
Hangzhou, China
hello.crabboss@gmail.com

Jiajun Zhou*

Institute of Cyberspace Security
Zhejiang University of Technology
Hangzhou, China

Binjiang Cyberspace Security Institute of ZJUT
Hangzhou, China
jjzhou@zjut.edu.cn

Qi Xuan

Institute of Cyberspace Security
Zhejiang University of Technology
Hangzhou, China

Binjiang Cyberspace Security Institute of ZJUT
Hangzhou, China
xuanqi@zjut.edu.cn

ABSTRACT

Graph neural networks (GNNs) have been proved powerful in graph-oriented tasks. However, many real-world graphs are heterophilous, challenging the homophily assumption of classical GNNs. To solve the universality problem, many studies deepen networks or concatenate intermediate representations, which does not inherently change neighbor aggregation and introduces noise. Recent studies propose new metrics to characterize the homophily, but rarely consider the correlation of the proposed metrics and models. In this paper, we first design a new metric, Neighborhood Homophily (NH), to measure the label complexity or purity in node neighborhoods. Furthermore, we incorporate the metric into the classical graph convolutional network (GCN) architecture and propose Neighborhood Homophily-based Graph Convolutional Network (NHGCN). In this framework, neighbors are grouped by estimated NH values and aggregated from different channels, and the resulting node predictions are then used in turn to estimate and update NH values. The two processes of metric estimation and model inference are alternately optimized to achieve better node classification. NHGCN achieves top overall performance on both homophilous and heterophilous benchmarks, with an improvement of up to 7.4% compared to the current SOTA methods.

CCS CONCEPTS

• **Computing methodologies** → **Neural networks.**

*Jiajun Zhou is the corresponding author.

Permission to make digital or hard copies of all or part of this work for personal or classroom use is granted without fee provided that copies are not made or distributed for profit or commercial advantage and that copies bear this notice and the full citation on the first page. Copyrights for components of this work owned by others than the author(s) must be honored. Abstracting with credit is permitted. To copy otherwise, or republish, to post on servers or to redistribute to lists, requires prior specific permission and/or a fee. Request permissions from permissions@acm.org.
CIKM '23, October 21–25, 2023, Birmingham, United Kingdom
© 2023 Copyright held by the owner/author(s). Publication rights licensed to ACM.
ACM ISBN 979-8-4007-0124-5/23/10...\$15.00
<https://doi.org/10.1145/3583780.3615195>

KEYWORDS

graph neural networks; node classification; homophily

ACM Reference Format:

Shengbo Gong, Jiajun Zhou, Chenxuan Xie, and Qi Xuan. 2023. Neighborhood Homophily-based Graph Convolutional Network. In *Proceedings of the 32nd ACM International Conference on Information and Knowledge Management (CIKM '23), October 21–25, 2023, Birmingham, United Kingdom*. ACM, New York, NY, USA, 5 pages. <https://doi.org/10.1145/3583780.3615195>

1 INTRODUCTION

Graph-structured data can effectively model real-world interactive systems and has been widely adopted as a modeling tool in fields such as finance and bioinformatics [8, 20], consequently speeding up the rapid development of graph neural networks (GNNs) for graph-oriented tasks. Classical GNNs [6, 10, 22] have been proved powerful in analyzing graph datasets that conform to the homophily assumption, where nodes tend to be connected to nodes with the same label. However, many real-world graphs contain heterophily or low homophily, e.g., normal users are usually associated with fraudulent accounts in financial fraud networks. Such scenarios do not follow the homophily assumption of classical GNNs, making them exposed to too much irrelevant information during message propagation and aggregation, leading to poor performance.

Such cases can be summarized as the universality problem [4], calling for a generic solution applicable to both homophilous and heterophilous graphs, i.e., universality necessitates that models function independently of homophily or heterophily assumptions.

Related Work. To go beyond the homophily, some spectral methods espouse the intuition that non-local information might be helpful [13]. Therefore, they resort to deeper GNNs, since stacking layers is equivalent to larger receptive field sizes, making nodes access to non-local information [4]. But the ensuing problems such as over-smoothing [12, 17] and model degradation [25] need to be alleviated by initial connection, skip connection, and linearization. Representative methods are GCNII [3], GPRGNN [4], BernNet [7]. Maintaining local assumptions, FAGCN [1] and ACM [15] design local filters to better capture local information. *However, limited by*

the globality of spectral theory, they are inherently unable to group information from different orders and thus introduce noise [23].

Spatial methods do not rely on spectral graph theory and thus allow fine-grained adaptations of message propagation rules. GeomGCN [18] and WRGAT [21] rewire the graphs to aggregate latent space neighbors or structurally similar neighbors. CPGNN [26] and HOG [23] reuse the predicted labels to calibrate the message propagation. *These methods require computing aggregating weights or new topologies and are thus time-consuming.*

Most related studies are GBK[5], GGCN [24] and ACM [15], since they also adopt a three-channel architecture in respective models. However, the first two are not directly from the definition of homophily, though they prove that their associations with homophily on an ad hoc assumption. The difference between ours and ACM is the selection of neighbors rather than low or high frequencies.

Motivation and Contributions. Most of existing methods ignore the fact that homophilous nodes behave differently with heterophilous nodes. But it can be commonly observed in real-world graphs, e.g., researchers in interdisciplinary studies favor citing literature from multiple fields, while others confine their references within a single discipline [2]. In such scenarios, mixing messages from “outward” and “inward” neighbors in the same channel can be considered an unwise practice. Furthermore, the classical metric falls short in common cases [16], and new homophily metrics are not well designed for guiding the model. Therefore, we propose a novel spatial domain approach – Neighborhood Homophily-based Graph Convolutional Network (NHGCN), in which neighbors are grouped by estimated NH , and nodes receive messages from low- and high- NH neighbors through different channels. **Our contributions are:** 1) proposing a new metric which can alleviate the dilemma of classical metric and guide the model from end-to-end; 2) devising a simple but effective model with a backbone of GCN; 3) our model achieves SOTA on 7 out of 10 popular datasets containing different level on homophily.

2 PRELIMINARIES

Notations. An attributed graph can be denoted as $G = (V, E, X, Y)$, where V and E are the sets of nodes and edges respectively, $X \in \mathbb{R}^{|V| \times f}$ is the node feature matrix, and $Y \in \mathbb{R}^{|V| \times C}$ is the node label matrix. Here we use $|V|$, f , C to denote the number of nodes, the dimension of the node features, and the number of node classes, respectively. Each row of X is the feature vector of node v_i , and each row of Y is the one-hot label of node v_i . The structure elements (V, E) can also be denoted as an adjacency matrix $A \in \mathbb{R}^{|V| \times |V|}$ that encodes pairwise connections between the nodes, whose entry $A_{ij} = 1$ if there exists an edge between v_i and v_j , and $A_{ij} = 0$ otherwise. Based on the adjacency matrix, we can define the degree distribution of G as a diagonal degree matrix $D \in \mathbb{R}^{|V| \times |V|}$ with entries $D_{ii} = \sum_{j=1}^{|V|} A_{ij} = d_i$ representing the degree value of v_i .

Graph Convolutional Network. GCN [10] can be formulated as:

$$B = \text{softmax} \left(\tilde{A} \cdot \text{ReLU} \left(\tilde{A} X W_0 \right) \cdot W_1 \right) \quad (1)$$

where the output B is the soft assignment of label predictions, and GCN-style regularization is:

$$\tilde{A} = (D + I)^{-1/2} (A + I) (D + I)^{-1/2} \quad (2)$$

Node Homophily. This metric is proposed in [18] and is widely used to measure the homophily, which can be defined as follows:

$$\begin{aligned} \text{node-level: } \mathcal{H}_i^{\text{node}} &= \frac{1}{d_i} \cdot |\{v_j \mid (v_i, v_j) \in E, y_i = y_j\}| \\ \text{graph-level: } \mathcal{H}_G &= \frac{1}{|V|} \sum_{v_i \in V} \mathcal{H}_i^{\text{node}} \end{aligned} \quad (3)$$

Node-level homophily denotes the proportion of direct neighbors that share the same label as the target node, whereas graph-level metric evaluates global homophily of a graph by averaging across all nodes. Most existing studies utilize graph-level homophily to distinguish between homophilous and heterophilous graphs, yet they overlook the significance at node level. Zhu et al. [27] first observed the *tick-like* phenomenon between node-level homophily and accuracies (See Fig. 2). UDGCN [14] first suggested that nodes with low or high homophily should be distinguished using the metric within one graph. Nevertheless, this classical metric falls short in many recent observations and is restricted to first-order neighborhoods, making it difficult to include more label information.

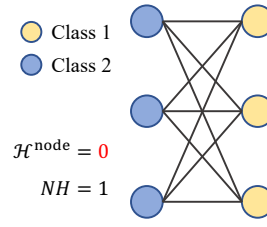


Figure 1: NH can measure the prediction ability of GCN but $\mathcal{H}^{\text{node}}$ fails.

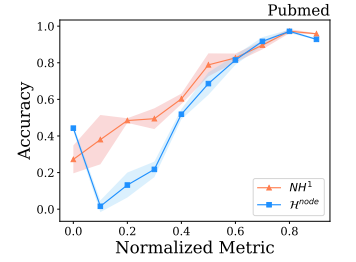


Figure 2: Correlation between accuracy of GCN and two metrics.

3 METHODOLOGY

3.1 Neighborhood Homophily Metric

Generally, heterophily is not conducive to classical GNNs because the features of different classes of nodes will be inappropriately mixed during message aggregation, leading to the learned node features being indistinguishable [27]. However, GCN still performs well on bipartite graphs that are completely heterophilous under the definition of the node homophily metric, bringing contradictory judgments [16]. As illustrated in Fig. 1, node homophily ($\mathcal{H}^{\text{node}} = 0$) cannot explain the fact that GCN still performs well on bipartite graphs. To overcome the shortcomings of classical homophily metrics, we propose a new metric termed Neighborhood Homophily (NH), which can measure the label complexity or purity in the neighborhoods of target nodes.

Definition. For a target node v_i , its k -hop neighborhood homophily NH_i^k can be defined as follows:

$$NH_i^k = \frac{|\mathcal{N}(i, k, c_{\max})|}{|\mathcal{N}(i, k)|} \quad \text{with } c_{\max} = \arg \max_{c \in [1, C]} |\mathcal{N}(i, k, c)| \quad (4)$$

where $\mathcal{N}(i, k) = \{v \mid (0 \text{ or } 1) \leq \text{ShortestPath}(v_i, v) \leq k\}$ means the neighbor set in the k -hop neighborhood of v_i , $\mathcal{N}(i, k, c) = \{v_j \mid$

$v_j \in \mathcal{N}(i, k, y_j = c)$ means the set of neighbors whose node label is c in the k -hop neighborhood of v_i . The hop k and whether $\mathcal{N}(i, k)$ includes the target node v_i (0 or 1) are treated as hyper-parameters. For an isolated node, we set its NH value to 1. The value domain of NH can be determined as $NH \in [1/C, 1]$, where the minimum and maximum values correspond to the most complex and purest neighborhoods, respectively.

In Fig. 1, $NH = 1$ indicates that the NH metric considers the neighborhoods of the nodes in the bipartite graph to have the lowest complexity (or the highest purity) and will not confuse GCN.

Comparison. Since classical GNNs such as GCN are designed based on homophily assumption, they naturally perform poorly in low homophily scenarios. Therefore, a well-designed homophily metric should behave consistently with the performance of GCN. To facilitate comparison between NH and the node homophily, we normalize these two metrics to unify their ranges to $[0, 1]$. Utilizing these two metrics, we divide all nodes into ten groups according to their metric levels, ranging from 0 to 1 in intervals of 0.1. The ordinate represents the intra-group accuracies on the standard GCN (2 layers with 64 hidden units, 0.5 dropout rate, and ReLU). As shown in Fig. 2, the accuracy curve represented by NH rises almost monotonically, reflecting that GCN performs better for prediction in scenarios with higher NH . However, GCN has abnormally high prediction accuracy for the nodes with the lowest node homophily. Such phenomena well illustrates that NH metric can better measure the difficulty of classifying nodes with GCN, i.e., NH is a better metric than node homophily. Meanwhile, we also compare the prediction results of our proposed model and GCN on different node groups, as shown in Fig. 5, from which we can see that with the guidance of NH metric, our model can better predict low homophily nodes while maintaining the prediction effect on high homophily nodes when compared with GCN.

3.2 Neighborhood Homophily Mask

The key design of NH metric is that it counts the label distribution, which is target-driven in the case of semi-supervised learning. Moreover, label distribution is the direct reason why graphs are categorized as homophilous or heterophilous. During the training phase, we follow a valid and common practice [26], that is, using the predicted labels partly complemented by ground-truth labels of the training set. We first initialize the NH values of all nodes to 1, and then update the NH values at each subsequent epoch when the validation accuracy achieves a new high. Each time the NH value are updated, we utilize a threshold T to separate the nodes into low- and high- NH ones, thereby enabling us to generate the Neighborhood Homophily Masks (NH mask):

$$m_i^{\text{low}} = \mathbb{I}(NH_i^k < T), \quad m_i^{\text{high}} = \mathbb{I}(NH_i^k \geq T) \quad (5)$$

where m^{low} (or m^{high}) $\in \mathbb{R}^{1 \times |V|}$ is mask vector. The absolute separation of nodes by setting threshold ensures the hard topology optimization, also used in [11, 28].

3.3 NH-based Message Propagation

As mentioned above, low- and high- NH nodes have different behavior patterns. Therefore, during message propagation, the low- and high- NH neighbors around target nodes should also transmit their

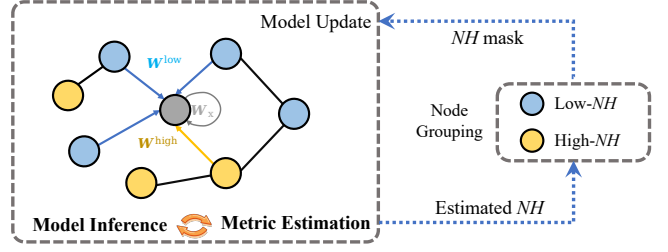


Figure 3: Illustration of NHGCN framework. Two alternating processes are: 1) each time the validation accuracy achieves a new high, estimate the NH values of nodes and update the NH masks, which can divide all nodes into two groups (low- and high- NH); 2) the two groups of nodes are asymmetrically aggregated in two different channels, and the raw node features are mapped in the third channel, and the outputs of the three channels are combined for subsequent model training.

messages from different channels. Here we design Neighborhood Homophily-based Graph Convolutional Network (NHGCN), which utilizes the NH masks to guide the message propagation. The backbone of NHGCN is a mask-based deformation of GCN architecture:

$$H^s = \tilde{A}_{\text{mask}} \cdot \text{ReLU}(\tilde{A}_{\text{mask}} \cdot XW_0^s) \cdot W_1^s, \quad A_{\text{mask}} = A \odot m^s \quad (6)$$

where $W_0^s \in \mathbb{R}^{f \times f'}$ and $W_1^s \in \mathbb{R}^{f' \times f'}$ are the weight matrices, f' is the hidden dimension, and $s \in \{\text{low}, \text{high}\}$ indicates different learning channels. Note that $A \odot m^s$ implies performing row-wise Hadamard product on A , which separates neighbors into two channels and adopt channel-specific weights. Then the masked adjacent matrix is regularized in a GCN-style as Equ. 2. Since the existence of isolated and neighbor-independent nodes, we introduce a third channel to preserve the raw features:

$$H_x = \text{ReLU}(XW_x) \quad (7)$$

where $W_x \in \mathbb{R}^{f \times f'}$ is the weight matrix. Finally, we combine the representations from the three channels and derive the soft assignment prediction $B \in \mathbb{R}^{n \times C}$ through a MLP as follows:

$$B = \text{softmax}\left(\left(\alpha_{\text{low}}H^{\text{low}} + \alpha_{\text{high}}H^{\text{high}} + \alpha_x H_x\right) \cdot W_o\right) \quad (8)$$

where $W_o \in \mathbb{R}^{f' \times C}$ is the weight matrix in the MLP, and $\alpha_{\text{low}} + \alpha_{\text{high}} + \alpha_x = 1$, where α are learnable scale weights initialed by $\frac{1}{3}$. Finally, we employ the cross-entropy as the classification loss.

4 EVALUATIONS

4.1 Experiment Setup

Datasets. We use 10 real-world datasets as in [4], among which the first five (*Cora*, *Citeseer*, *Pubmed*, *Computers* and *Photo*) are homophilous datasets and the last five (*Chameleon**, *Squirrel**, *Actor*, *Cornell* and *Texas*) are heterophilous ones. Specifically, *Chameleon** and *Squirrel** are de-duplicated version to get rid of the risk of data leakage provided by [19]. We adopt dense split as [4], i.e., 60% / 20% / 20% for training / validation / testing set.

Table 1: Results on real world benchmark datasets: Mean Test Accuracy (%) \pm Standard Deviation. The best result on each dataset is marked in bold while the second best is underlined. Time consumption implies the average time per run on Cora.

| | Cora | Citeseer | Pubmed | Photo | Computers | Actor | Chameleon* | Squirrel* | Cornell | Texas | Time/s |
|------------------|------------------------------------|------------------------------------|------------------------------------|------------------------------------|------------------------------------|------------------------------------|------------------------------------|------------------------------------|------------------------------------|------------------------------------|--------|
| <i>MLP</i> | 73.74 \pm 1.73 | 76.85 \pm 1.11 | 86.86 \pm 0.51 | 91.28 \pm 0.63 | 84.35 \pm 1.02 | 36.82 \pm 1.19 | 31.99 \pm 4.11 | 44.61 \pm 4.23 | 80.98 \pm 7.01 | 82.34 \pm 5.12 | 0.56 |
| <i>GCN</i> | 87.50 \pm 1.56 | 81.11 \pm 1.06 | 88.08 \pm 0.50 | 93.94 \pm 0.47 | 89.72 \pm 0.43 | 33.15 \pm 1.75 | 42.63 \pm 3.64 | 47.83 \pm 2.90 | 79.18 \pm 3.94 | 88.24 \pm 1.50 | 0.37 |
| <i>GPRGNN</i> | 89.46 \pm 1.40 | 81.84 \pm 1.08 | <u>90.46 \pm 0.75</u> | 94.62 \pm 0.45 | 89.35 \pm 1.33 | 39.22 \pm 1.17 | <u>45.15 \pm 4.95</u> | 45.85 \pm 2.33 | 90.66 \pm 4.58 | 88.72 \pm 6.50 | 1.35 |
| <i>ACMGCN</i> | 87.80 \pm 1.23 | 82.05 \pm 1.26 | 90.40 \pm 0.29 | <u>95.04 \pm 0.44</u> | <u>90.31 \pm 0.39</u> | 39.09 \pm 1.42 | 43.74 \pm 4.03 | 39.64 \pm 7.84 | 91.48 \pm 2.29 | 88.09 \pm 3.20 | 0.96 |
| <i>FAGCN</i> | 88.90 \pm 0.88 | 80.78 \pm 0.95 | 89.16 \pm 0.67 | 94.89 \pm 0.48 | 87.61 \pm 1.17 | <u>40.90 \pm 1.12</u> | 45.20 \pm 4.45 | <u>53.28 \pm 1.28</u> | 88.52 \pm 4.95 | <u>89.57 \pm 3.94</u> | 1.60 |
| <i>GGCN</i> | 87.34 \pm 1.15 | 78.95 \pm 1.77 | 89.03 \pm 0.43 | 91.26 \pm 0.80 | 75.98 \pm 7.68 | 38.86 \pm 0.80 | 40.70 \pm 4.00 | 49.31 \pm 4.62 | 90.66 \pm 3.28 | 83.40 \pm 6.91 | 6.18 |
| <i>GBK</i> | 88.69 \pm 0.42 | 79.18 \pm 0.96 | 85.49 \pm 0.61 | 81.61 \pm 8.05 | 81.20 \pm 5.62 | 37.27 \pm 0.98 | 45.32 \pm 4.61 | 45.41 \pm 3.19 | 81.08 \pm 4.88 | 74.27 \pm 2.18 | 105.08 |
| <i>WRGAT</i> | 88.20 \pm 2.26 | 76.81 \pm 1.89 | 89.13 \pm 0.53 | 92.23 \pm 0.64 | 86.13 \pm 0.76 | 37.91 \pm 1.63 | 42.46 \pm 3.71 | 45.47 \pm 3.56 | 83.62 \pm 5.50 | 81.62 \pm 3.90 | 25.39 |
| <i>NHGCN</i> | 89.05 \pm 1.24 | <u>81.87 \pm 1.20</u> | 91.56 \pm 0.50 | 95.35 \pm 0.34 | 90.72 \pm 0.34 | 43.94 \pm 1.14 | 47.60 \pm 4.15 | 54.38 \pm 1.17 | 91.28 \pm 3.94 | 93.11 \pm 2.42 | 3.68 |
| <i>w/o group</i> | 88.62 \pm 1.70 | 81.31 \pm 1.10 | 90.09 \pm 0.92 | 94.67 \pm 0.33 | 89.21 \pm 0.77 | 39.67 \pm 0.75 | 41.17 \pm 7.21 | 53.28 \pm 2.43 | 89.36 \pm 4.60 | 87.23 \pm 4.26 | 3.33 |

Baselines. We compare NHGCN with three categories of eight baselines: 1) basic methods: two-layer MLP, GCN [10]; 2) spectral methods: GPRGNN [4], ACMGCN [15], FAGCN [1]; 3) spatial methods: GGCN [24], GBK [5], WRGAT [21].

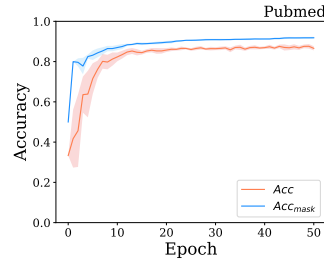
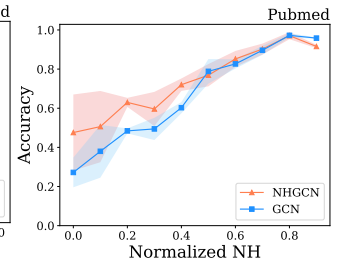
Settings. We report the average results and running time of 10 runs fixed by 10 random seeds in Table 1. For all baselines, we reproduce them with their open-sourced code. For all methods, we set optimizer to Adam [9], hidden dimension to 512, the maximum epochs to 500 with 100 epochs patience for early stopping. The search space for learning rate, weight decay and dropout rate will be shared among all methods. We only have specific hyperparameters k chosen from $\{1, 2\}$, $if_include_self$ when calculate NH , and the threshold T chosen from $\{1/2, 1/C\}$ with 0.5 internals for the reciprocal (maximal is set to 4). The source code of NHGCN is available at <https://github.com/rockcor/NHGCN>.

4.2 Analysis

Node Classification. Table 1 reports the node classification results on ten benchmarks, from which we can observe and conclude: 1) Compared with eight latest competitors, our NHGCN shows top average ranking, indicating that our methods are effective and have better universality for datasets with different level of homophily. More specifically, our method achieves SOTA on 7 out of 10 benchmarks with relatively low time consumption and variance, guaranteeing the efficiency and stability. In particular, we achieved 7.4% improvement on the *Actor*, significantly higher than all existing GNNs to our best knowledge. 2) Baselines show preferences for different datasets. Generally, spectral methods performs better on datasets with high homophily, while spatial methods performs better on datasets with high heterophily. In addition, most spatial methods run with an unacceptable time consumption.

Ablations. When our grouping strategy is removed, NHGCN degenerates to a combination of GCN output and raw features, represented by *w/o group* for short. Other components such as layers and combiner is the same as NHGCN. The results are shown in the last row of Tab. 1. When comparing NHGCN with *w/o group*, it is well illustrated that treat neighbors differently is an effective scheme.

Metric Effectiveness. Our grouping strategy is totally based on the NH metric. However, the NH is calculated by the predicted labels. To find out if NH really plays a role in our model, and if the co-optimization achieved, we plot the accuracies of the estimated NH along with the node classification, as shown in Fig. 4. During

**Figure 4: Accuracy of node classification and masks.****Figure 5: Accuracy of two models in varying NH .**

training, the two lines rise in synchrony, proving that the two accuracies are interdependence and the two processes are co-optimized. **Debiasing Potential.** Fig. 5 shows that NHGCN surpasses GCN at almost all NH levels, thus it can achieve better overall accuracy on *Pubmed*. This suggests that our grouping strategy benefits low- NH nodes more than high- NH ones. From perspective of debiasing learning [14], it significantly reduces the accuracy gap between low- and high- NH nodes, ensuring that classification performance is relatively maintained even if the proportion of nodes in these two groups changes. In practice, this also means that our model is fair to both “outward” and “inward” nodes. Such phenomena are also reflected in other datasets.

5 CONCLUSIONS

In this paper, we address two common problems of GNNs tailored for graph universality problem: 1) The model training process is not well associated with their proposed metrics; 2) High time consumption for both model training and metric calculating. We design neighborhood homophily, as an easy-to-compute metric to measure the homophily, which overcomes the shortness of classical metrics. By a slight transformation of GCN, our metric can guide message propagation in a grouping strategy, simply but effectively.

ACKNOWLEDGMENTS

This work was partially supported by the Key R&D Programs of Zhejiang, China under Grant No. 2022C01018, by the Zhejiang Provincial Natural Science Foundation of China under Grants No. LR19F030001, and by the National Natural Science Foundation of China under Grant No. 61973273.

REFERENCES

- [1] Deyu Bo, Xiao Wang, Chuan Shi, and Huawei Shen. 2021. Beyond low-frequency information in graph convolutional networks. In *AAAI*.
- [2] Lutz Bornmann and Hans-Dieter Daniel. 2008. What do citation counts measure? A review of studies on citing behavior. *Journal of documentation* (2008).
- [3] Ming Chen, Zhewei Wei, Zengfeng Huang, Bolin Ding, and Yaliang Li. 2020. Simple and deep graph convolutional networks. In *ICLR*. PMLR, 1725–1735.
- [4] Eli Chien, Jianhao Peng, Pan Li, and Olgica Milenkovic. 2021. Adaptive Universal Generalized PageRank Graph Neural Network. In *ICLR*.
- [5] Lun Du, Xiaozhou Shi, Qiang Fu, Xiaojun Ma, Hengyu Liu, Shi Han, and Dongmei Zhang. 2022. GBK-GNN: Gated Bi-Kernel Graph Neural Networks for Modeling Both Homophily and Heterophily. In *WWW*. 1550–1558.
- [6] Will Hamilton, Zhitao Ying, and Jure Leskovec. 2017. Inductive representation learning on large graphs. In *NeurIPS*, Vol. 30.
- [7] Minguo He, Zhewei Wei, Hongteng Xu, et al. 2021. Bernnet: Learning arbitrary graph spectral filters via bernstein approximation. In *NeurIPS*, Vol. 34. 14239–14251.
- [8] Mengda Huang, Yang Liu, Xiang Ao, Kuan Li, Jianfeng Chi, Jinghua Feng, Hao Yang, and Qing He. 2022. Auc-oriented graph neural network for fraud detection. In *WWW*. 1311–1321.
- [9] Diederik P Kingma and Jimmy Ba. 2014. Adam: A method for stochastic optimization. *arXiv preprint arXiv:1412.6980* (2014).
- [10] Thomas N Kipf and Max Welling. 2017. Semi-supervised classification with graph convolutional networks. In *ICLR*.
- [11] Johannes Klicpera, Stefan Weissenberger, and Stephan Günnemann. 2019. Diffusion improves graph learning. In *NeurIPS*. 13366–13378.
- [12] Qimai Li, Zhichao Han, and Xiao-Ming Wu. 2018. Deeper insights into graph convolutional networks for semi-supervised learning. In *AAAI*.
- [13] Meng Liu, Zhengyang Wang, and Shuiwang Ji. 2021. Non-local graph neural networks. *IEEE Transactions on Pattern Analysis and Machine Intelligence* (2021).
- [14] Yang Liu, Xiang Ao, Fuli Feng, and Qing He. 2022. Ud-gnn: Uncertainty-aware debiased training on semi-homophilous graphs. In *SIGKDD*. 1131–1140.
- [15] Sitao Luan, Chenqing Hua, Qincheng Lu, Jiaqi Zhu, Mingde Zhao, Shuyuan Zhang, Xiao-Wen Chang, and Doina Precup. 2022. Revisiting Heterophily For Graph Neural Networks. In *NeurIPS*.
- [16] Yao Ma, Xiaorui Liu, Neil Shah, and Jiliang Tang. 2021. Is Homophily a Necessity for Graph Neural Networks?. In *ICLR*.
- [17] Kenta Oono and Taiji Suzuki. 2019. Graph Neural Networks Exponentially Lose Expressive Power for Node Classification. In *ICLR*.
- [18] Hongbin Pei, Bingzhe Wei, Kevin Chen-Chuan Chang, Yu Lei, and Bo Yang. 2019. Geom-GCN: Geometric Graph Convolutional Networks. In *ICLR*.
- [19] Oleg Platonov, Denis Kuznedelev, Michael Diskin, Artem Babenko, and Liudmila Prokhorenkova. 2023. A critical look at the evaluation of GNNs under heterophily: Are we really making progress?. In *ICLR*.
- [20] Jonathan M Stokes, Kevin Yang, Kyle Swanson, Wengong Jin, Andres Cubillos-Ruiz, Nina M Donghia, Craig R MacNair, Shawn French, Lindsey A Carfrae, Zohar Bloom-Ackermann, et al. 2020. A deep learning approach to antibiotic discovery. *Cell* 180, 4 (2020), 688–702.
- [21] Susheel Suresh, Vinit Budde, Jennifer Neville, Pan Li, and Jianzhu Ma. 2021. Breaking the limit of graph neural networks by improving the assortativity of graphs with local mixing patterns. In *SIGKDD*.
- [22] Petar Veličković, Guillem Cucurull, Arantxa Casanova, Adriana Romero, Pietro Lio, and Yoshua Bengio. 2018. Graph attention networks. In *ICLR*.
- [23] Tao Wang, Di Jin, Rui Wang, Dongxiao He, and Yuxiao Huang. 2022. Powerful graph convolutional networks with adaptive propagation mechanism for homophily and heterophily. In *AAAI*.
- [24] Yujun Yan, Milad Hashemi, Kevin Swersky, Yaoqing Yang, and Danai Koutra. 2022. Two sides of the same coin: Heterophily and oversmoothing in graph convolutional neural networks. In *ICDM*. IEEE, 1287–1292.
- [25] Wentao Zhang, Zeang Sheng, Ziqi Yin, Yuezhian Jiang, Yikuan Xia, Jun Gao, Zhi Yang, and Bin Cui. 2022. Model Degradation Hinders Deep Graph Neural Networks. In *SIGKDD*.
- [26] Jiong Zhu, Ryan A Rossi, Anup Rao, Tung Mai, Nedim Lipka, Nesreen K Ahmed, and Danai Koutra. 2021. Graph neural networks with heterophily. In *AAAI*.
- [27] Jiong Zhu, Yujun Yan, Lingxiao Zhao, Mark Heimann, Leman Akoglu, and Danai Koutra. 2020. Beyond homophily in graph neural networks: Current limitations and effective designs. In *NeurIPS*, Vol. 33. 7793–7804.
- [28] Minhao Zou, Zhongxue Gan, Ruizhi Cao, Chun Guan, and Siyang Leng. 2023. Similarity-navigated graph neural networks for node classification. *Information Sciences* 633 (2023), 41–69.